JOURNAL OF GUIDANCE, CONTROL, AND DYNAMICS
Vol. 21, No. 2, March–April 1998

Engineering Notes

ENGINEERING NOTES are short manuscripts describing new developments or important results of a preliminary nature. These Notes cannot exceed 6 manuscript pages and 3 figures; a page of text may be substituted for a figure and vice versa. After informal review by the editors, they may be published within a few months of the date of receipt. Style requirements are the same as for regular contributions (see inside back cover).

Radiotelescope Low-Rate Tracking Using Dither

Wodek Gawronski* and Ben Parvin†
Jet Propulsion Laboratory,
California Institute of Technology,
Pasadena, California 91109

Introduction

MANY radiotelescopes cannot precisely point at a certain part (about 5%) of the sky that requires tracking with very low-azimuth angular rates (approximately 0.4 mdeg/s or lower). For such slow rates, dry rolling friction is observed at the telescope drives that cause an unwanted increase of pointing error. (Pointing error is defined as a difference between the target location and the rf beam position.)

In this Note we analyze the National Radio Astronomy Observatory's Green Bank Telescope located in West Virginia. It is one of the world's two largest articulated radiotelescopes. (Its 100-m-diam main reflector is of the same size as the reflector of the Effelsberg radiotelescope in Germany.) The Green Bank Telescope has a unique configuration characterized by the offset reflector. The telescope's size, weight, and especially configuration create difficulties in precision tracking. One of the difficulties is observed during tracking at low rates. Namely, for rates lower than 0.3 mdeg/s a nonsmooth telescope motion with breakaways may occur. The peak-to-peak pointing error due to friction is 1.4 mdeg.

A high-frequency external signal injected into a system (its frequency much higher than the system dynamics) is called a dither.[1,2] It has long been known that injection of high-frequency signals into a nonlinear system results in eliminating the system limit cycles.[1–3] This phenomenon was detected in electrical circuits by Appleton in 1922. Although dither is a well-known remedy for the nonlinear behavior of control systems, little is known of its impact on the dynamics of large flexible structures. The purpose of this Note is to show that dither improves the telescope pointing at low tracking rates. We will show that the high-frequency dither signal excites local vibrations only (at the wheels) causing the breaking of the friction–stiction phenomena. The vibrations are not transmitted through the telescope structure, thus not impacting its pointing performance. Also, this Note presents a friction model frequently used in the antenna industry. It includes the velocity threshold and the determination of the applied torque within the threshold.

Dry Friction Model

The telescope's nonlinear dynamics, at low rates, is caused by the dry friction phenomenon. Friction is a torque, or a force, that depends on the relative velocity of the moving surfaces. In the coulomb friction model it is constant after the motion begins, and this constant value is called the coulomb friction torque. At zero speed, the friction torque is equal and opposite to the applied torque, unless the latter one is larger than the stiction torque. In this case, the friction torque is equal to the stiction torque. The stiction torque is a torque at the moment of breakaway and is larger than the coulomb torque. A diagram of the friction torque vs relative velocity is shown in Fig. 1.

Many friction models have been developed; for example, Refs. 1 and 4–7. They reflect different aspects of the friction phenomena, and their usefulness depends on application purposes. The model presented here combines basic physical properties of the dry friction with the numerical features that improve digital simulations. Its accuracy for the antenna tracking purposes has been tested at many existing telescopes and antennas. In this model, v is the telescope wheel velocity and $v_t > 0$ is a wheel velocity threshold, which is a small positive number. T_c is the coulomb friction torque, and T_s the stiction torque; then the friction torque model T is defined as follows:

$$T = \begin{cases} -T_c \operatorname{sign}(v) & \text{for} \quad |v| > v_t \\ -\min(|T_d|, T_s) \operatorname{sign}(T_d) & \text{for} \quad |v| \le v_t \end{cases} \tag{1}$$

where $\operatorname{sign}(v) = 1, 0,$ and -1 for $v > 0$, $v = 0$, and $v < 0$, respectively; and T_d is the total applied torque. In this model, if the surfaces in a contact develop a measurable relative velocity, such that $|v| > v_t$, the friction torque is constant, directed opposite to the relative speed. If the relative velocity is small, namely, within the threshold ($|v| \le v_t$), the torque does not exceed the stiction torque and the applied torque and is directed opposite to the applied torque. The velocity threshold v_t is implemented for numerical purposes because numerically the zero state does not exist.

It follows from Eq. (1) that to determine the friction torque T one has to know the coulomb friction torque T_c, the stiction (breakaway) torque T_s, the applied torque T_d, the wheel rate v, and the wheel rate threshold v_t. The variables are determined as follows.

The coulomb friction torque is proportional to force F, which is normal to the surface:

$$T_c = \mu r F \tag{2}$$

where r is the wheel radius and μ is the friction coefficient. For hard steel $\mu = 0.0012$–0.002.

The stiction (breakaway) torque T_s is most often assumed to be 20–30% higher than the coulomb friction, that is,

$$T_s = \alpha T_c \qquad \text{where} \qquad \alpha = 1.2\text{–}1.3 \tag{3}$$

The total applied torque T_d is determined from the plant dynamics as follows. Let the discrete state-space equation of the plant (which includes the telescope structure and its drives) be

$$x(i+1) = A_d x(i) + B_{dr} r(i) + B_{df} T(i) \tag{4a}$$

$$v(i+1) = C_d x(i+1) \tag{4b}$$

In this model, Δt is sampling time, i is the ith sample, $v(i)$ is the wheel rate at time instant $i\Delta t$, $x(i)$ is the plant state at the instant $i\Delta t$, $r(i)$ is the telescope angular input rate, and $T(i)$ is the friction azimuth torque. Additionally, A_d is the telescope discrete-time state matrix, B_{dr} and B_{df} are telescope rate and friction torque input matrices, and C_d is the wheel rate output matrix (for more about

Received May 22, 1997; presented as Paper 97-3749 at the AIAA Guidance, Navigation, and Control Conference, New Orleans, LA, Aug. 11–13, 1997; revision received Oct. 29, 1997; accepted for publication Nov. 2, 1997.

*Senior Member of Technical Staff, Communications Ground Systems Section.

†Project Element Manager, Avionic Systems Engineering Section.

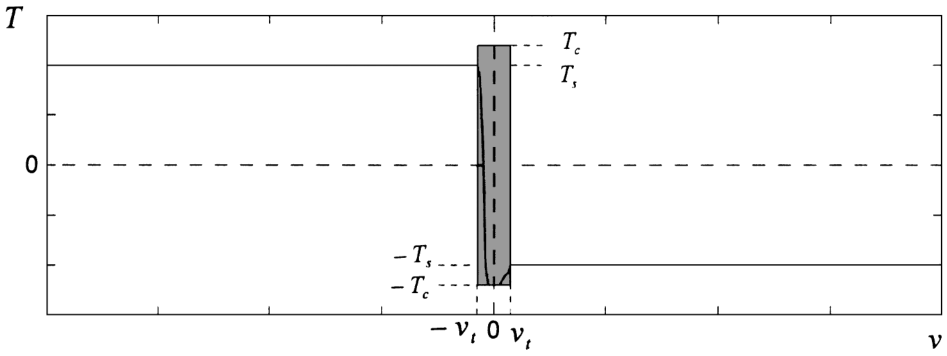

Fig. 1 Friction torque vs rate.

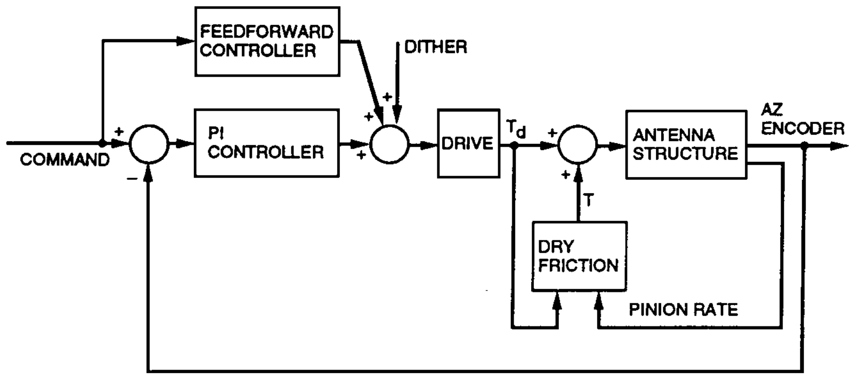

Fig. 2 Azimuth control system with dry friction and dither.

telescope dynamics, see Ref. 8). Left multiplying Eq. (4a) by C_d gives

$$v(i+1) = C_d x(i+1) = C_d A_d x(i) + C_d B_{dr} r(i) + C_d B_{df} T(i) \tag{5}$$

According to the friction model, for the wheel rate being within the threshold, i.e., such that $|v(i+1)| \leq v_t$, one obtains $v(i+1) = 0$; thus, from Eq. (5) one obtains

$$T(i) = -\frac{C_d}{C_d B_{df}}[A_d x(i) + B_{dr} r(i)] \tag{6}$$

and the applied torque T_d has sign opposite to the preceding friction torque T.

The wheel rate threshold v_t was assumed to be 0.67 mdeg/s.

Explaining Dither Action Using Linearized Model

There are many ways to reduce the system dynamics due to friction. Most of them are based on closed-loop compensation.[1,2,9–11] Here, we apply an open-loop technique by dithering the driving torque. The block diagram of the closed-loop system with the dry friction and the rate dither is shown in Fig. 2. In this diagram, according to Eq. (1), the dry friction torque T is a nonlinear function of the azimuth wheel rate v and the drive torque T_d.

To describe the dither action we consider the torque at the azimuth wheel. For low rates, the driving torque T_d is smaller than the dry friction torque T_c, causing the telescope to stop. While resting, the error between the commanded position and the actual telescope position increases. In the closed-loop configuration the increased error causes an increase in the driving torque T_d, and eventually the movement of the telescope is observed. The cycle repeats itself and is called limit cycling. The plots of the telescope pointing error and the pinion angle in this limit cycling are shown in Figs. 3a and 3b (solid line).

A harmonic dither of amplitude d_0 and period t_0, $d(t) = d_0 \sin(2\pi t/t_0)$ is introduced at the telescope rate input. When dither is implemented, the torque level at the wheel is raised. This increase is not a constant one: it varies harmonically. If the amplitude of the driving torque T_d exceeds the friction torque, the telescope is moving continuously and the limit cycling is overcome. Because of the high frequency of the dither signal (high when compared with the telescope dynamics), the harmonic movement is a local phenomenon at the wheels. It is not propagated through the telescope structure and has very low impact on the structural dynamics and, consequently, on the telescope pointing.

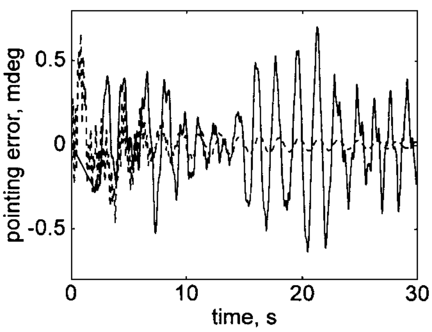

a) Pointing error

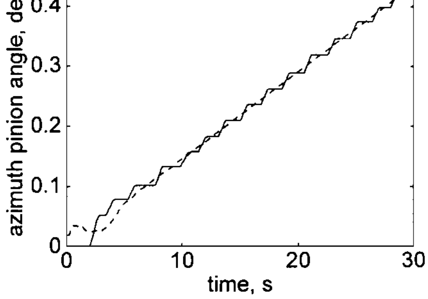

b) Azimuth pinion angle

Fig. 3 Simulated trackings: ——, no dither and - - -, with dither.

The preceding heuristic explanation of the dither action can be derived more formally. Consider the continuous-time telescope model with the nonlinear friction torque $T(v)$, driven by the command rate r and dither d:

$$\dot{x} = Ax + B_r(r + d) + B_f T(v), \qquad v = Cx \tag{7}$$

The parameters (A, B_r, B_f, C) are the continuous-time counterparts of the discrete-time parameters $(A_d, B_{dr}, B_{df}, C_d)$ as in Eq. (4), and $x(t)$ is the state variable of the plant. This equation is averaged over the dither period t_0. The average value x_a of x is defined as

$$x_a(t) = \frac{1}{t_0}\int_t^{t+t_0} x(\tau)\,\mathrm{d}\tau \tag{8}$$

Note that in Eq. (7) the average value of the rate command is almost the same as the instantaneous value because the command changes insignificantly over the period t_0, i.e., $r(t) \cong r(t + t_0)$. The average value $\hat{T}(v)$ of the nonlinear torque $T(v)$ is obtained from the dry friction torque as in Eq. (1). The velocity threshold v_t in this equation is assumed to be zero. (The nonzero threshold was introduced earlier to avoid numerical difficulties in simulations.) Thus, the wheel friction torque is given as $T = -T_c\,\mathrm{sign}(v + d)$. The average torque $\hat{T}$ is called the smooth image of the dry friction torque. The smooth image $\hat{T}$ is defined as

$$\hat{T} = \frac{1}{t_0}\int_t^{t+t_0} T\,\mathrm{d}\tau$$

therefore, one obtains

$$\hat{T}(v) = \frac{1}{t_0}\int_t^{t+t_0} T(v)\,\mathrm{d}\tau = -\frac{1}{t_0}\int_t^{t+t_0} T_c\,\mathrm{sign}(v + d)\,\mathrm{d}\tau$$

$$= -\frac{2T_c}{\pi}\arcsin\left(\frac{v}{d_0}\right) \tag{9}$$

The plot of $\hat{T}$ with respect to v/d_0 for $T_c = 1$ is shown in Fig. 4. One can see from Fig. 4 that, although the dry friction T is a discontinuous function of the rate, its smooth image $\hat{T}$ is, by definition, a smooth function of the rate. It also follows from Fig. 4 that the smooth image exists only for the dither amplitudes that extend the wheel rate, i.e., for $d_0 > v$. This is quite understandable because for the dither amplitude smaller than the wheel rate there is no change in the friction torque.

Because the function $\hat{T}$ is smooth, it can be linearized for small rate variations. Consequently, for small wheel rate v that is proportional to the rate of the command r, $v = k_r r$, one obtains

$$\hat{T}(d_0) \cong k_0 r, \qquad k_0 = -\frac{2T_c k_r}{\pi d_0} \tag{10}$$

The plot of linearized $\hat{T}$ in Fig. 4 (dashed line) reveals a good coincidence with $\hat{T}$ for $v < 0.5 d_0$.

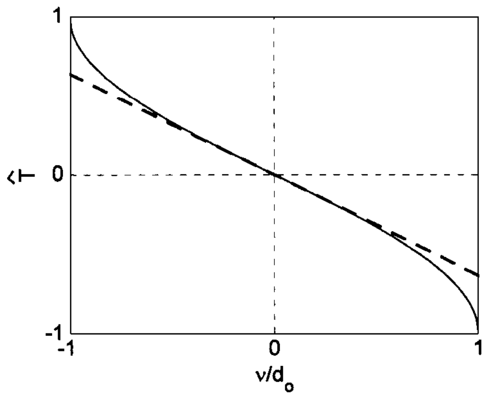

Fig. 4 Smooth image of dry friction (——) and linearized image (– – –).

Introducing Eq. (10) to the averaged Eq. (7), one obtains the following linear system:

$$\dot{x}_a = Ax_a + B_{r0}r + B_r d, \qquad y_a = Cx_a \tag{11}$$

with the input matrix B_{r0} in the form $B_{r0} = B_r + k_0 B_n$. The latter equation proves that the system dynamics with dither is a linear one. Also, notice that the dither input has no significant impact at the telescope pointing. Let us write the pointing y_a as a superposition of the pointing (y_{ar}) due to the input r and the pointing (y_{ad}) due to the dither input d, i.e., $y_a = y_{ar} + y_{ad}$. Notice that the dither is of high frequency; therefore, the response y_{ad} is negligible when compared with y_{ar}; thus, $y_a \cong y_{ar}$. The latter shows that the dither action makes the telescope dynamics linear but it does not show itself at the output; thus, the telescope pointing performance is not affected.

Nonlinear Simulation Results

Typically, the dither signal should be injected just ahead of the nonlinearity. In the case of the Green Bank Telescope it is a rate command at the telescope azimuth drives. In this case the dither is simply added to the feedforward command generated by the controller computer.

The dither amplitude and frequency are determined as follows. The frequency must be much higher than the telescope dynamics. Because no significant telescope dynamics is observed above 10 Hz, the dither frequency 30 Hz is chosen. The dither amplitude depends on the level of friction torque. Dry friction torque for tracking at a rate of 0.3 mdeg/s is smaller than 5600 N-m. For this friction level the dither amplitude was selected to be 0.18 deg/s using the telescope pointing simulations with various dither amplitudes and showing that the pointing error was the smallest for the dither of amplitude 0.18 deg/s. The plot of the pointing error for this dither amplitude is shown in Fig. 3a (broken line). The plot shows that the steady-state pointing error dropped 18-fold, from 1.4 to 0.08 mdeg. The pinion now moves smoothly, as shown in Fig. 3b (broken line).

Acknowledgments

The authors would like to thank Robert Hall and Lee King of the National Radio Astronomy Observatory, Charlottesville, Virginia, for valuable discussions.

References

[1] Armstrong-Helouvry, B., Dupont, P., and Canudas de Wit, C., "A Survey of Models, Analysis Tools and Compensation Methods for the Control of Machines with Friction," *Automatica*, Vol. 30, No. 7, 1994, pp. 1083–1138.

[2] Dupont, P. E., and Dunlap, E. P., "Friction Modeling and PD Compensation at Very Low Velocities," *Journal of Dynamic Systems, Measurement and Control*, Vol. 117, No. 1, 1995, pp. 8–14.

[3] Lee, S., and Meerkov, S. M., "Generalized Dither," *International Journal of Control*, Vol. 53, No. 3, 1983, pp. 741–747.

[4] Armstrong-Helouvry, B., Dupont, P., and Canudas de Wit, C., "Friction in Servo Machines: Analysis and Control Methods," *Applied Mechanics Review*, Vol. 47, No. 7, 1994, pp. 275–305.

[5] Bliman, P.-A. J., "Mathematical Study of the Dahl's Friction Model," *European Journal of Mechanics, A/Solids*, Vol. 11, No. 6, 1992, pp. 835–848.

[6] Canudas de Wit, C., Olsson, H., Astrom, K. J., and Lischinsky, P., "A New Model for Control of Systems with Friction," *IEEE Transactions on Automatic Control*, Vol. 40, No. 3, 1995, pp. 419–425.

[7] Dahl, P. R., "Solid Friction Damping of Mechanical Vibrations," *AIAA Journal*, Vol. 14, No. 12, 1976, pp. 1675–1682.

[8] Gawronski, W., and Mellstrom, J. A., "Control and Dynamics of the Deep Space Network Antennas," *Control and Dynamics Systems*, edited by C. T. Leondes, Vol. 63, Academic, San Diego, CA, 1994, pp. 289–412.

[9] Cai, L., and Song, G., "Joint Stick-Slip Friction Compensation of Robot Manipulators by Using Smooth Robust Controllers," *Journal of Robotic Systems*, Vol. 11, No. 6, 1994, pp. 451–469.

[10] Dupont, P. E., "Avoiding Stick-Slip Through PD Control," *IEEE Transactions on Automatic Control*, Vol. 39, No. 5, 1994, pp. 1094–1097.

[11] Southward, S. C., Radcliffe, C. J., and MacCluer, C. R., "Robust Nonlinear Stick-Slip Friction Compensation," *Journal of Dynamic Systems, Measurement and Control*, Vol. 113, No. 4, 1991, pp. 639–645.